

Biocompatible Characteristics of Sulfobetaine-Containing Brush Polymers

Jin Chul Kim^{†,1}, Mihee Kim^{†,1}, Jungwoon Jung^{†,1}, Heesoo Kim^{*,2}, Ik Jung Kim²,
Jung Ran Kim³, and Moonhor Ree^{*,1}

¹Department of Chemistry, Division of Advanced Materials Science, Center for Electro-Photo Behaviors in Advanced Molecular Systems, Pohang Accelerator Laboratory, BK School of Molecular Science, and Polymer Research Institute, Pohang University of Science & Technology, Gyeongbuk 790-784, Korea

²Department of Microbiology, and Dongguk Medical Institute, Dongguk University College of Medicine, Gyeongbuk 780-714, Korea

³Department of Pathology, and Dongguk Medical Institute, Dongguk University College of Medicine, Gyeongbuk 780-714, Korea

Received October 10, 2011; Revised November 15, 2011; Accepted November 18, 2011

Abstract: A series of well-defined brush polymers, poly(oxy(11-(3-sulfonylpropyltrimethyl-glyciny)undecylesterthiomethyl)ethylene-co-oxy(*n*-dodecylthio-methyl)ethylene)s (PECH-DMAPSm, where *m* is the mol% of the DMAPS [sulfobetaine] end group) were synthesized. The thermal properties and phase transitions of these polymers were investigated. The polymers were thermally stable up to 185 °C and were found to form favorably into multilayer structures, always providing hydrophilic, zwitterionic sulfobetaine end groups at the film surface. Because of the presence of these sulfobetaine groups at the surface, the polymer films promoted HEP-2 cell adhesion and revealed biocompatibility in mice but significantly suppressed protein adsorption. These results collectively indicate that the sulfobetaine-containing brush polymers are suitable for use in biomedical applications, including medical devices and biosensors that require biocompatibility.

Keywords: brush polymer, sulfobetaine, self-assembly, water sorption, water contact angle, protein adsorption, cell adhesion, biocompatibility.

Introduction

Biomaterials have gained much attention because of their demands in medical implants and devices, as well as in tissue culture and drug delivery.^{1,2} However, they often elicit inflammatory responses, including foreign body responses and fibrous encapsulation.^{1,2} Also dynamic adsorption of proteins and other biomolecules onto the implanted biomaterials are issued because they can cause inflammatory cell responses.² Thus, much effort has been made to develop of biomaterials with improved biocompatibility. One of the most widely used approaches to improving the biocompatibility has been the incorporation of biomimetic molecules into materials.²⁻⁴ To incorporate biomimetic groups, several methods have been reported so far: (i) the formation of biomimetic group containing polymer brushes on material surfaces,^{2,5-9} (ii) the formation of self-assembled monolayers (SAMs) of biomimetic molecules on material surfaces,^{2,10-15}

and (iii) the preparation of graft, comb-like, random and block copolymers bearing biomimetic groups.¹⁶⁻²⁰ However, each method has some drawbacks. Furthermore, the achievement of surfaces rich with biomimetic groups is not trivial goal. Therefore, the development of biomaterials with biomimetic group-rich surfaces that can provide excellent biocompatibility remains in the exploration stage.

In particular, sulfobetaine has a chemical structure similar to that of 2-aminoethanesulfonic acid or taurine which is present in high concentrations in animals and occurs in traces in plants.^{8,21} Poly(ethylene glycol) (PEG) is well known as a biomaterial because of the biocompatibility.⁵ In this study we have thus attempted to incorporate sulfobetaine to the bristle ends of a brush polymer based on the PEG backbone. We synthesized newly poly(oxy(11-(3-sulfonylpropyltrimethylglyciny)-undecylesterthiomethyl)ethylene-co-oxy(*n*-dodecylthiomethyl)ethylene)s (PECH-DMAPSm, where *m* is the mol% of the DMAPS end group) (Scheme I). Due to the ethylene oxide backbone and zwitterionic sulfobetaine moieties, the polymers showed relatively high water sorption, depending on the composition. The polymers containing ≥ 80 mol% sulfobetaine moiety were found to be completely

*Corresponding Authors. E-mails: ree@postech.edu or hskim@dongguk.ac.kr

[†]J. C. Kim, M. Kim, and J. Jung contributed equally to this study.

soluble in water. Film structures of the polymer were examined by grazing incidence X-ray scattering using synchrotron radiation sources. This scattering analysis found that the polymers can self-assemble and then form a molecular multi-bilayer (*i.e.*, layer-by-layer) structure, always providing a sulfobetaine rich surface. Due to the sulfobetaine rich surface, the polymer films suppressed protein adsorption and furthermore exhibited good cell adhesion and biocompatibility in mice.

Experimental

Synthesis of Brush Polymers. A polyepichlorohydrin (PECH) was synthesized from epichlorohydrin by ring-opening polymerization as described in the literature.¹⁹ The obtained PECH polymer was confirmed by proton and carbon nuclear magnetic resonance (¹H and ¹³C NMR) spectroscopy (model AM300, Bruker, Rheinstetten, BW, Germany) and infrared (IR) spectroscopy (model Research Series 2, ATI Mattson, Lakewood, NJ, USA). The polymer was determined to have a weight-average molecular weight M_w of 38,500 and a number-average molecular weight M_n of 22,700 by a gel permeation chromatography (model PL-GPC 210, Polymer Labs, Amherst, MA, USA) calibrated with polystyrene standards.

To the chloromethylenyl side groups of the PECH polymer, two different kinds of brushes in various compositions were introduced as shown in Scheme I. Namely, a series of poly(oxy(11-hydroxyundecylthiomethyl)ethylene-*co*-oxy(*n*-dodecylthiomethyl)ethylene)s (PECH-OHm) were prepared from the reaction of the PECH polymer with sodium 11-hydroxyundecylthiolate and sodium *n*-dodecylthiolate in various mole fractions as described previously in the literature.^{19,22} For a typical synthetic example, the preparation of PECH-OH100 polymer is described as follows. A mixture of PECH (3.380 g, 36.50 mmol) and sodium 11-hydroxyundecylthiolate (9.074 g, 39.70 mmol) in 40 mL of dimethylacetamide (DMAc) was stirred at room temperature. After 24 h the reaction solution was poured into 100 mL chloroform and then the used DMAc solvent was eliminated by washing with water several times. The solution was dried over anhydrous magnesium sulfate and filtered off. The filtrate was concentrated under reduced pressure. The obtained polymer product was poured into cold *n*-hexane and then the polymer product in white powder was filtered, followed by drying in vacuum. For the polymer product, the incorporation of 11-hydroxyundecyl groups was confirmed to be 100% by NMR spectroscopy. ¹H NMR (300 MHz, CDCl₃, δ (ppm)): 3.70-3.59 (br, 3H, OCH, OCH₂), 2.75-2.52 (m, 4H, CH₂SCH₂), 1.57-1.13 (m, 18H, CH₂); ¹³C NMR (75 MHz, CDCl₃, δ (ppm)): 79.36-78.72, 63.07, 39.23, 33.26, 32.82, 29.75-28.53, 25.76; IR (in film, ν (cm⁻¹)): 3590-3100 (alcohol, O-H stretch), 2960 and 2854 (methylene, C-H stretch), 1500-1400 (CH₂ bending), 1110 (ether, C-O-C stretching), and 732 (thioether, C-S-C stretching).

The obtained PECH-OHm polymers were further converted to poly(oxy(11-(dimethylglyciny)undecylthiomethyl)ethylene-*co*-oxy(*n*-dodecylthiomethyl)ethylene)s (PECH-DMGm) according to a method reported previously.¹⁹ For a typical synthetic example, the preparation of PECH-DMG100 polymer is described here. PECH-OH100 (0.260 g, 1.00 mmol OH), *N,N'*-dimethylglycine (0.120 g, 1.20 mmol), *N*-(3-dimethylaminopropyl)-*N'*-ethylcarbodiimide hydrochloride (EDC, 0.465 g, 3.00 mmol) and 4-(dimethylamino)pyridine (DMAP, 0.183 g, 1.50 mmol) were dissolved in dichloromethane (20 mL) and stirred at room temperature for 24 h. The solvent was removed by evaporation and residue was purified by column chromatography with dichloromethane eluent. The product in yellow viscous liquid was obtained. ¹H NMR (300 MHz, CDCl₃, δ (ppm)): 4.12 (t, 2 H), 3.87-3.57 (br, 3H), 3.16 (t, 2H), 2.84-2.42 (m, 4 H), 2.35 (s, 6 H), 1.73-1.00 (m, 18H); ¹³C NMR (75 MHz, CDCl₃, δ (ppm)): 170.79, 79.36-78.72, 63.07, 53.2, 44.1, 39.23, 33.26, 32.82, 29.75-28.53, 25.76; IR (in film, ν (cm⁻¹)): 2960 and 2854 (C-H stretch), 1730 (ester, C=O stretch), 1500-1400 (CH₂ bending), 1270-1160 (ester, O-C, stretch), 1200-1150 (C-N, stretch), 1110 (ether, C-O-C stretching), 732 (thioether, C-S-C stretching).

The obtained PECH-DMGm polymers were again converted to the final product, poly(oxy(11-(3-sulfonylpropyltrimethylglyciny)undecylesterthiomethyl)ethylene-*co*-oxy(*n*-dodecylthiomethyl)ethylene)s (PECH-DMAPSm) by reaction with 1,3-propanesultone. For example, the preparation of PECH-DMAPS100 polymer is described as follows. PECH-DMG100 (0.350 g, 1.00 mmol) was dissolved in acetone (2 mL). 1,3-Propanesultone (0.150 g, 1.20 mmol) was added to the solution and stirred for 24 h. The product was obtained as white precipitate. The product was filtrated and washed with acetone several times, followed by drying in vacuum. ¹H NMR (300 MHz, DMSO-*d*₆, δ (ppm)): 4.43 (t, 2 H), 4.15 (t, 2 H), 3.86-3.42 (br, 3H), 3.19 (t, 6 H), 2.77-2.32 (m, 4 H), 2.32 (m, 2 H), 2.04 (m, 2 H), 1.73-1.00 (m, 18H); ¹³C NMR (75 MHz, DMSO-*d*₆, δ (ppm)): 170.71, 66.58, 64.93, 61.44, 51.72, 47.83, 45.13, 29.75-28.53, 28.70, 26.11, 19.89; IR (in film, ν (cm⁻¹)): 2960 and 2854 (C-H stretch), 1730 (ester, C=O stretch), 1500-1400 (CH₂ bending), 1250-1160 (ester, O-C, stretch), 1190-1110 (C-N, stretch), 1200-1160 (ether, C-O-C stretching), 1040 (SO₃ stretch), and 732 (thioether, C-S-C stretching).

Characterizations. Thermal stability and phase transitions of PECH-DMAPSm polymers were measured with a rate of 10.0 °C/min under nitrogen atmosphere by thermogravimetry (TGA; model TG/DGA-6300, Seiko Instrument, Tokyo, Japan) and differential scanning calorimetry (DSC) (model DSC-220CU, Seiko Instrument, Tokyo, Japan).

For each brush polymer, solutions of various concentrations (0.2-1.0 wt%) were prepared in chloroform and filtered using disposable syringes equipped with a polytetrafluoroethylene filter of pore size 0.2 μ m. The filtered solutions were deposited on various substrates (silicon wafers, glass

slides, poly(ethylene terephthalate) (PET) sheets (300 μm thick), and gold-coated glass prisms (BaK4, barium crown glass) by spin- or dip-coating process and then dried at 50 $^{\circ}\text{C}$ for 1 day under vacuum. Thicknesses of the obtained films were determined to range 15-100 nm by ellipsometry (model M-2000, Woollam, Lincoln, NE, USA) and α -stepper analysis (model Tektak3, Veeco Co., Plainview, NY, USA). In aqueous media, the PECH-DMPS100 and PECH-DMAPS80 films were found to be completely soluble in aqueous media while the other films containing ≤ 60 mol% of DMAPS bristles were sustained their film shape. Thus, all experiments associated with aqueous media were conducted for the brush polymers containing ≤ 60 mol% of DMAPS bristles.

Grazing incidence X-ray scattering (GIXS) measurements were carried out at the 4C2 beamline of the Pohang Accelerator Laboratory at Pohang University of Science & Technology according to a method as described previously in the literature.²³⁻²⁶ The film samples, which were coated with 40-50 nm thickness on Si substrates, were measured at a sample-to-detector distance of 129.8 and 2,110 mm, using an X-ray radiation source of 0.138 nm wavelength and a two-dimensional (2D) charge-coupled detector (CCD; Roper Scientific, Trenton, NJ, USA). The samples were mounted on a home-made z -axis goniometer equipped with a vacuum. The incident angle α_i of the X-ray beam was set at 0.140 $^{\circ}$, which is between the critical angles of the films and the Si substrate ($\alpha_{c,f}$ and $\alpha_{c,s}$). All GIXS measurements were carried out at 20 $^{\circ}\text{C}$. Each measurement was collected for 30-60 s.

Water sorptions of the brush polymer films (80-100 nm thickness on silicon substrates) were measured in phosphate buffered saline (PBS; pH=7.4) for 4 h by using a spectroscopic ellipsometer (model M-2000) equipped with a liquid cell. PECH-DMAPS80 and PECH-DMAPS100 were excluded due to their solubility in aqueous media. The window angle of the liquid cell was set to 75 $^{\circ}$, which is perpendicular to the incidence angle. In addition static water contact angle measurements were conducted for the brush polymer films using a contact angle meter (KSV Instruments, Tokyo, Japan).

Protein Adsorption. Fibrinogen (bovine), lysozyme (chicken egg), albumin (bovine serum) and γ -globulin (bovine) were purchased from Sigma. Protein adsorptions to the brush polymer films were measured at 25 $^{\circ}\text{C}$ using an SPR spectrometer (K-MAC, Daejeon, Korea) with a monochromatic laser light source at a wavelength of 780 nm. Brush polymer films (15-20 nm thickness) except PECH-DMAPS80 and PECH-DMAPS100 were coated on glass prisms deposited with 50 nm thick gold layer. Protein solutions (1 mg/mL in PBS) were injected for 10 min at a flow rate of 7.5 $\mu\text{L}/\text{min}$ and then replaced by PBS for 2 min.

Cell Adhesion. Films of the brush polymers except PECH-DMAPS80 and PECH-DMAPS100 were prepared with 80-100 nm thickness by dip-coating on glass slides as described.^{19,27,28} HEp-2 cell line was received from the Korea Cell Line Bank (Seoul, Korea). Cell culture media and reagents were pur-

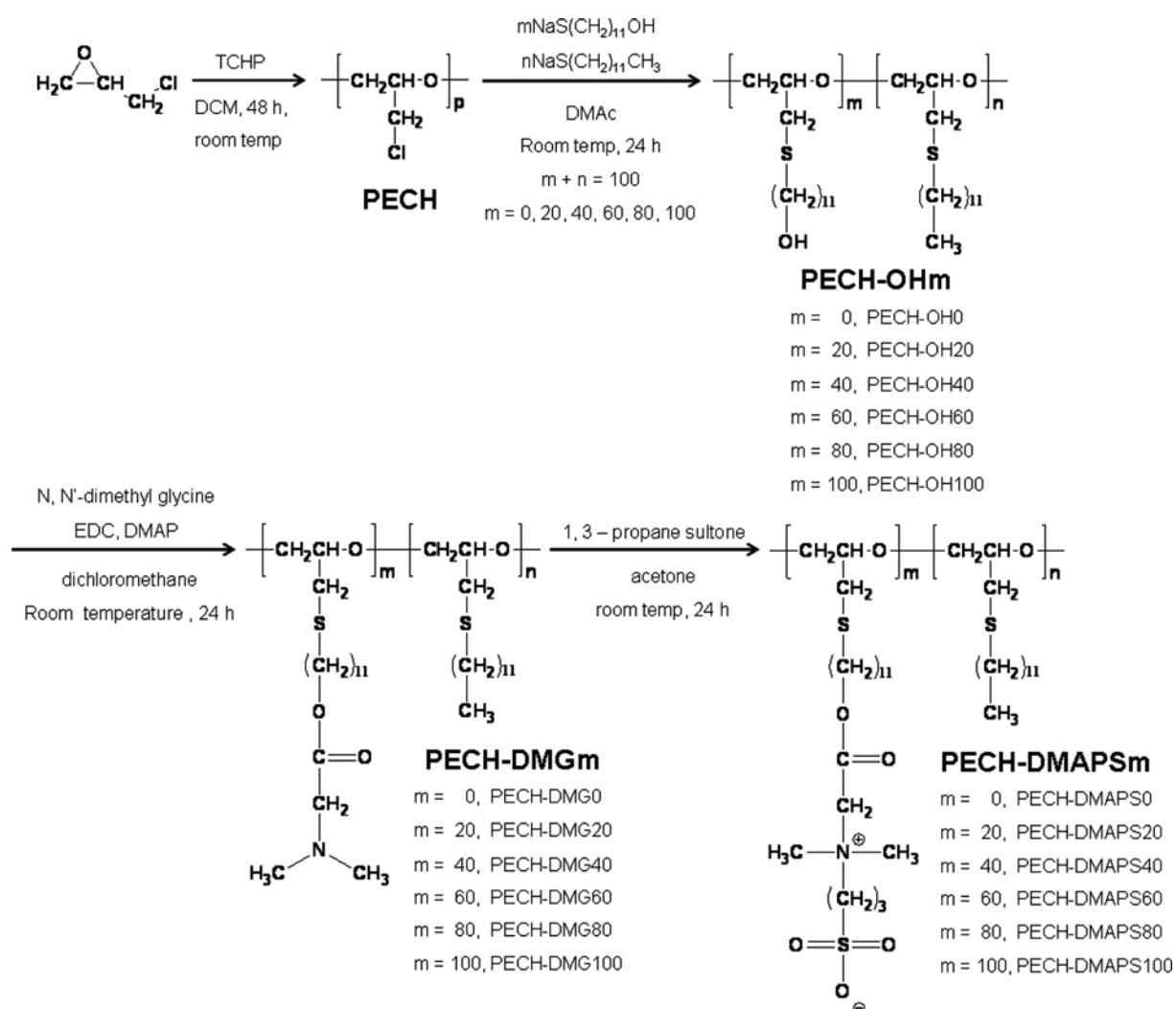
chased from Invitrogen (Grand Island, NY, USA). HEp-2 cell adhesion was tested on the brush-polymer films. The cell growth was checked up to 6 days using an inverted microscope (model ECLIPSS TS 100, Nikon, Tokyo, Japan) equipped with a digital camera.

Implantation. ICR mice were purchased from Korea Research Institute of Bioscience & Biotechnology (Daejeon, Korea). The mouse experiment was reviewed and approved by Animal Care/Ethics of Dongguk University College of Medicine and maintained according to the university guidelines for the care and use of animals. The PECH-DMAPS0 and PECH-DMAPS40 polymer films (dip-coated on PET discs of 0.7 cm diameter) were disinfected by immersion in 100% ethyl alcohol for 20 min and 70% ethyl alcohol for 20 min, and rinsed with sterile saline solution (0.9%) for 1 h. The mouse implantation experiments were performed as described previously.^{19,27,28} The implanted polymer films and surrounding tissues were removed at 1, 2, 4, and 8 week post implantation for morphological examination and histological analyses to assess tissue reactions.

Results and Discussion

A PEG based polymer, PECH was successfully synthesized with a reasonably high molecular weight by the ring-opening polymerization of epichlorohydrin. From this polymer, a series of PECH-based brush polymers (PECH-OHm: m=0%, 20%, 40%, 60%, 80%, and 100%, which are the mol% of hydroxyl end group in the bristle ends) were prepared by the reactions of its chloro groups with sodium salts of 11-mercapto-1-undecanol and mercaptododecane in various portions (Scheme 1). The synthesized PECH-OHm polymers were characterized by ^1H and ^{13}C NMR spectroscopy as well as IR spectroscopy. For example, the representative ^1H NMR and IR spectra of PECH-OH100 are shown in Figures 1(a) and 2(a), respectively. The ^1H NMR spectroscopy analysis confirmed that these bristles were incorporated with 100% yield into the PECH polymers. In this analysis, there were used the proton peaks at 2.75-2.52 ppm ($-\text{CH}_2\text{SCH}_2-$ unit in the bristle), 1.57-1.13 ppm ($-(\text{CH}_2)_9-$ unit in the bristle), and 3.70-3.59 ppm ($-\text{OCH}-$ and $-\text{OCH}_2-$ units in the backbone). The presence of hydroxyl groups in the bristles was further confirmed by IR spectroscopy. Furthermore, for each PECH-OHm polymer, the proportions of the two different incorporated bristles were determined from the proton peaks around 0.90 ppm ($-\text{CH}_3$ end group in the *n*-dodecylthiomethyl bristle) and at 2.75-2.52 ppm ($-\text{CH}_2\text{SCH}_2-$ unit in the bristles).

For the obtained PECH-OHm polymers, N,N' -dimethylglycines were incorporated by reaction to the hydroxyl groups at the bristle ends, giving the target product, PECH-DMGm. This esterification and its reaction yield were confirmed by NMR spectroscopy (Figure 1(b)). In the analysis, there were used the proton peaks at 4.12 ppm ($-\text{C}(\text{O})\text{CH}_2\text{N}=\text{unit}$ in the



Scheme I. Synthetic route of the brush polymers with various numbers of bristle ends incorporating DMAPS moieties, PECH-DMAPS_m; here it is noted that PECH-OH₀, PECH-DMG₀, and PECH-DMAPS₀ are the same brush polymer bearing only *n*-dodecyl part in the bristle.

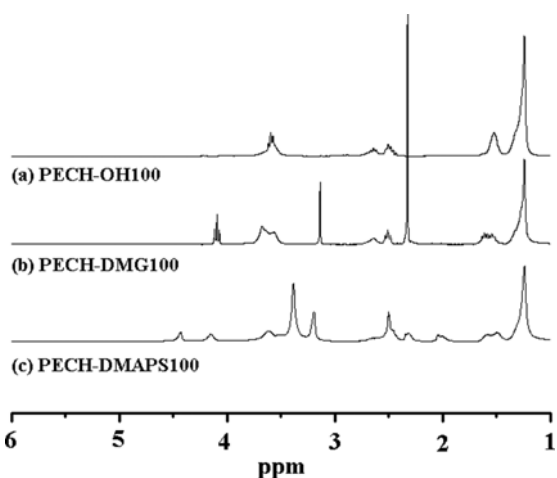


Figure 1. Representative ^1H NMR spectra of the synthesized polymers.

bristle) and 1.57–1.13 ppm ($-(\text{CH}_2)_9$ -unit in the bristle). This NMR analysis found that the esterification reaction took place with 100% yield. Furthermore, in the ^{13}C NMR spectroscopy analysis, the characteristic peaks of the incorporated *N,N'*-dimethylglycyl unit were confirmed: 170.79 ($=\text{O}$), 53.2 ($-\text{N}(\text{CH}_3)_2$) and 44.1 ppm ($-\text{N}(\text{CH}_3)_2\text{CH}_2\text{C}(=\text{O})\text{O}-$). The IR spectroscopy also identified the vibrational characteristics of the incorporated *N,N'*-dimethylglycyl unit: 1730 cm^{-1} (stretching, $-\text{CH}_2\text{C}(=\text{O})\text{O}-$) and 1231 cm^{-1} (stretching, $-\text{CH}_2\text{N}-$) (Figure 2(b)). Moreover, no presence of hydroxyl groups was confirmed for the product.

For the obtained PECH-DMG_m polymers, the incorporated *N,N'*-dimethylglycyl ends were further reacted with 1,3-propanesultone molecules, converting to the sulfobetaine moieties. In the ^1H NMR spectrum of the reaction product, the signal of $-\text{CH}_3$ in the amine end group at 2.35 ppm completely disappeared (Figure 1(c)). Instead, a new peak appeared

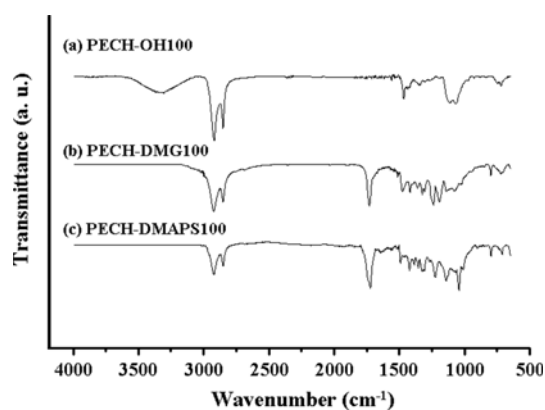


Figure 2. Representative IR spectra of the synthesized polymers.

at 3.19 ppm, which corresponds to $-\text{CH}_3$ in the sulfobetaine moiety. In addition, several characteristic peaks of the sulfobetaine-containing bristle were identified at 4.43 ppm ($-\text{O}-\text{C}(=\text{O})-\text{CH}_2-\text{N}(\text{CH}_3)_2^-$), 2.32 ppm ($-\text{CH}_2-\text{SO}_3^-$), and 2.04 ppm ($-\text{CH}_2-\text{CH}_2-\text{SO}_3^-$). Moreover, the ^{13}C NMR spectroscopy confirmed the sulfobetaine moiety incorporated into the bristle end groups: 51.72 ppm ($-\text{N}^+(\text{CH}_3)_2-$ and $-\text{CH}_2-\text{SO}_3^-$) and 19.89 ppm ($-\text{CH}_2-\text{CH}_2-\text{CH}_2-\text{SO}_3^-$). The IR spectrum showed a sharp peak at 1040 cm^{-1} (Figure 2(c)), which is attributed to SO_3^- vibration. The analysis results collectively confirmed that in the reaction the N,N' -dimethylglycyl end groups in the bristles were converted to the sulfobetaine moieties with 100% yield, producing the final target polymer, PECH-DMAPS m .

The brush polymers were found to be thermally stable over the range $185\text{--}220\text{ }^\circ\text{C}$, depending on the brush composition. Higher sulfobetaine (*i.e.*, DMAPS) content in the brush polymer revealed relatively lower thermal stability. The glass transition temperature T_g also varied with the mole fraction of DMAPS bristle ends over the temperature range -35 to $-27\text{ }^\circ\text{C}$; a higher DMAPS bristle end content in the

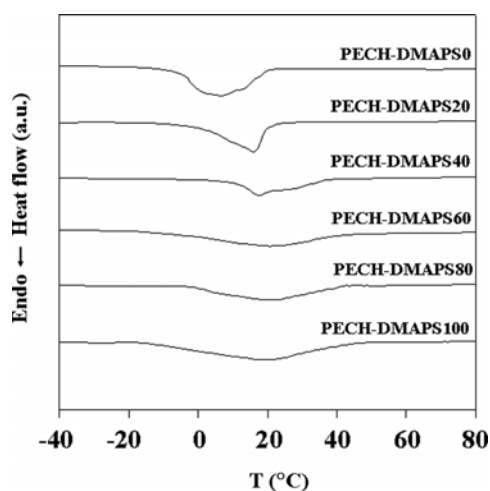


Figure 3. DSC thermograms of the PECH-DMAPS m polymers, which were measured at a rate of $10.0\text{ }^\circ\text{C}/\text{min}$ under nitrogen atmosphere.

polymer resulted in a lower T_g (Figure 3). PECH-DMAPS0 exhibited an additional endothermic peak centered at $6\text{ }^\circ\text{C}$, which is attributed to the melting of the ordered alkyl bristles (Figure 3). PECH-DMAPS100 also revealed an additional endothermic peak centered at $20\text{ }^\circ\text{C}$ (Figure 3). The brush polymers having 20–80 mol% DMAPS end group showed endothermic peak at temperatures between the melting points of PECH-DMAPS0 and PECH-DMAPS100. These results indicate that for the brush polymers, the bristles containing DMAPS (*i.e.*, sulfobetaine moiety) end are still able to make ordering.

Figure 4 shows representative 2D GIXS patterns, which were measured for films (40–50 nm thick) of PECH-DMAPS0 and PECH-DMAPS100. The PECH-DMAPS20 polymer revealed scattering pattern similar to that of the PECH-DMAPS0 polymer, whereas the other polymers showed scattering patterns similar to that of the PECH-DMAPS100 polymer (data not shown). The PECH-DMAPS0 film reveals two weak spots ($\alpha_f = 3.81^\circ$ and 5.70°) along the α_f direction at $2\theta_f = 0^\circ$, in addition to two scattering rings at 3.13° and 17.60° ($=2\theta_f$) (Figure 4(a)). The observation of these two spots indicated that a multilayer structure was present in the film. However, their intensities are weak, suggesting that the portion of such multilayer structure in the film is relatively lower. The two spots were determined to have d -spacings of 2.08 and 1.39 nm, which correspond to the second and third order reflections of the multilayer structure respectively. From these d -spacing data, the layer thickness in the multilayer structure was estimated to be 4.16 nm. This layer thickness is slightly larger than twice the length (1.80 nm) of the fully extended alkyl bristles; here the bristle length was estimated by performing a molecular simulation with the Cerius² software package (Accelrys). These results inform that the alkyl brushes in the multilayer structure have no interdigitation. On the other hand, the two ring scatterings at

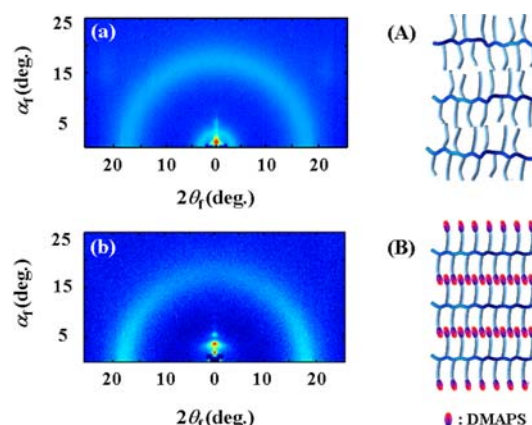


Figure 4. 2D GIXS patterns of the brush polymer thin films coated on silicon substrates at $20\text{ }^\circ\text{C}$: (a) PECH-DMAPS0; (b) PECH-DMAPS100. The measurements were carried out with $\alpha_f = 0.14^\circ$ in vacuum. Structural models proposed for the brush polymer films: (A) PECH-DMAPS0; (B) PECH-DMAPS100.

$2\theta_f = 3.13^\circ$ and 16.78° appeared apparently isotropic rather than anisotropic (Figures 4(a)), confirming that the polymer film was composed of a multi-bilayer structure phase as a minor component, and an amorphous phase as a major component. The amorphous halo rings were determined to have d -spacings of 2.53 and 0.47 nm, which correspond to the mean interdistances between the brush polymer chains and between the bristles respectively.

In comparison, the PECH-DMAPS100 polymer showed that the scattering spots along the α_f direction at $2\theta_f = 0^\circ$ are stronger in intensity (Figure 4(b)). The appearance of these scattering spots indicated that, in the films, the brush polymer molecules formed a multi-bilayer structure whose layers were stacked normal to the film plane. The layer thickness of the multi-bilayer structure was determined to be 4.40 nm, which is smaller than twice the length (2.84 nm) of the fully extended bristles, indicating that the bristles of the adjacent layers were partly interdigitated. The polymer film revealed a weak isotropic ring scattering and an anisotropic arc in the high angle region (Figures 4(b)). The very weak isotropic halo ring centered at $2\theta_f = 16.86^\circ$ (d -spacing=0.47 nm) might be attributed to the mean lateral interdistance of the polymer backbones in the amorphous phase, whereas the anisotropic arc centered at 17.13° - 17.67° ($2\theta_f$) (0.45-0.46 nm d -spacing) might derive from the mean lateral interdistance of the bristles participating in the multi-bilayer structure. Due to the formation of multi-bilayer structure, the polymer film provides sulfobetaine rich surface.

From the X-ray scattering results, structural models were proposed for the brush polymer films (Figure 4(A) and (B)). Films of the sulfobetaine-containing brush polymers always provided a surface rich with zwitterionic sulfobetaine end groups.

For the polymer films, static water contact angle measurements were conducted at 25°C . This analysis found that the polymer films exhibited water contact angles of 40.10° - 112.23° , depending on the brush composition: 112.23° ($\pm 1.21^\circ$) for PECH-DMAPS20, 40.10° ($\pm 0.25^\circ$) for PECH-DMAPS40, and 70.12° ($\pm 0.80^\circ$) for PECH-DMAPS60. Higher content of sulfobetaine moiety in the brush polymer revealed lower water contact angle. The results collectively indicate that the brush polymer containing $\leq 20\%$ sulfobetaine moiety is hydrophobic while the polymer with $>20\%$ sulfobetaine moiety is hydrophilic.

In addition, for the polymer films, the thickness change due to water sorption was measured in PBS at 25°C by ellipsometry. For an immersion time of 4 h, the PECH-DMAPS0 and PECH-DMAPS20 films exhibited very small variations in film thickness. However, for the PECH-DMAPS40 and PECH-DMAPS60 films the thicknesses were increased to 130%-163% of the initial value. These results indicate that the incorporation of DMAPS end groups with hydrophilic and zwitterionic characteristics enhanced the water sorption ability of the brush polymer. However, the incorporation of

20 mol% DMAPS was insufficient to enhance the water sorption of the brush polymer.

With the above structure and physiochemical characteristics, the brush polymer films were further tested for protein adsorption, cell adhesion and implantation.

Proteins adsorbed onto the surface of biomaterials can recruit factors related to thrombosis and blood coagulation, leading to life-threatening situations or causing functional failure when biomaterials are used in artificial organs, blood vessels, and other medical devices in contact with blood. Thus, protein adsorption tests on the brush polymer films were carried out with major plasma proteins (albumin, γ -globulin and fibrinogen) and lysozyme in PBS at room temperature by using SPR spectroscopy. Figure 5 shows the adsorption behaviors of proteins on the brush polymer films. On the PECH-DMAPS0 films, all the proteins showed various levels of adsorption: lysozyme adsorption occurred quickly to a high level; albumin and γ -globulin revealed low levels; fibrinogen adsorbed rather slowly to the highest level. However, protein adsorptions on the PECH-DMAPS20 films were significantly suppressed to very low levels except for lysozyme still exhibiting an intermediate level. Moreover, there are no protein adsorptions at all on the films of PECH-DMAPS40 and PECH-DMAPS60. The sulfobetaine group is zwitterionic and hydrophilic, easily being hydrated with water molecules. Thus, the sulfobetaine end groups present at the film surface of the brush polymers are favorably surrounded with water molecules in aqueous media, consequently providing an environment unfavorable for protein adsorption. Higher population of such sulfobetaine end groups at the film surface makes the surface resist to protein adsorption. The experimental results indicate that even 20

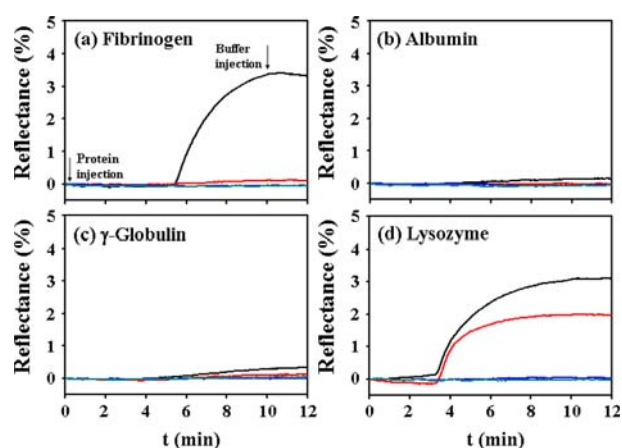


Figure 5. Reflectance variations of the brush-polymer films measured during protein adsorption by SPR spectroscopy at a fixed angle where the film reveals the minimum light reflectance: black line, PECH-DMAPS0; red, PECH-DMAPS20; blue, PECH-DMAPS40; green, PECH-DMAPS60. Protein solution in PBS (1 mg/mL) was injected for 10 min and then replaced by deionized water for 2 min.

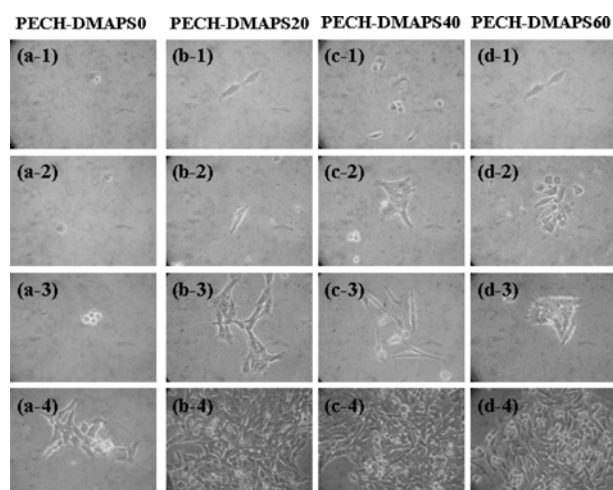


Figure 6. HEp-2 cell adhesion to the brush polymer films: (a-1)~(d-1), 1 day; (a-2)~(d-2), 2 days; (a-3)~(d-3), 3 days; (a-4)~(d-4), 6 days. The cell adhesion and growth in a humidified 5% CO₂ atmosphere at 37 °C were monitored up to 6 days. Original magnifications were 400×.

mol% sulfobetaine groups incorporated into the brush polymer can significantly suppress protein adsorption and further the incorporation of ≥ 40 mol% sulfobetaine groups prevents protein adsorption. Therefore, the sulfobetaine bristle containing brush polymers have very low possibility of blood coagulation when they are used for implantation.

The adhesion, growth, and proliferation of HEp-2 cells on the film surfaces of the brush polymers were evaluated for 6 days after seeding. As shown in Figure 6, HEp-2 cells started to adhere to the DMAPS containing film surfaces at 1 day. After 3 days, cell growth and division appeared normal on all the films of PECH-DMAPS20, 40, 60 brush polymers, while scarce cell growth was observed on the PECH-DMAPS0 film surface. The cells adhered to the DMAPS bristle-containing brush polymer films formed monolayers to reach confluence by 6 days. Therefore, it can be concluded that PECH-DMAPS20, PECH-DMAPS40, and PECH-DMAPS60 surfaces favorably supported not only the anchorage of mammalian cells but also their successful division and proliferation, compared with the PECH-DMAPS0. The excellent adhesion of cells on the DMAPS containing brush polymer films might be originated from the hydrophilic, zwitterionic sulfobetaine bristle end groups at the film surface and their hydration with water molecules.

One of the most important criteria for biomaterials in contact with human blood or tissues is whether they exhibit biocompatibility without causing any harm to the body.^{1,2} The importance of biocompatibility in determining the therapeutic value of biomaterials and in ensuring the efficacy and safety of implanted devices is well recognized.²⁹ To investigate biocompatibility of the PECH-DMAPS40 polymer compared with PECH-DMAPS0, subcutaneous implantation was

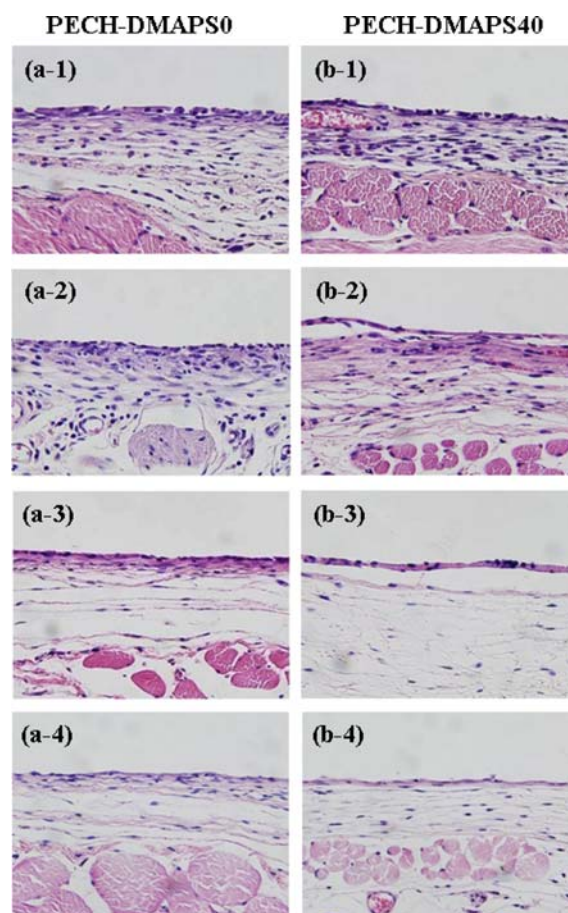


Figure 7. Tissue reactions at various times after implantation of the brush polymers: (a-1)~(b-1), 1 week; (a-2)~(b-2), 2 weeks; (a-3)~(b-3), 4 weeks; (a-4)~(b-4), 8 weeks. The films were dislodged during the staining process and thus not shown at the upper part of each figure. Original magnifications were 400×.

performed in mice. The implanted polymer films were removed with surrounding tissues at 1, 2, 4, and 8 weeks after implantation. Figure 7 shows representative optical micrographs of the subcutaneous tissue responses to the films. It is well known that acute inflammation is triggered by not only surgical injury but the implanted materials and that the subsequently released inflammatory mediators recruit neutrophils (one of the first responders) to the inflammation sites. When inflammation persists for weeks or longer, however, acute inflammation becomes chronic with prolonged accumulation of lymphocytes and macrophages which form giant cells around foreign bodies. As expected, many neutrophils and some giant cells were observed at 1 week with capsules starting to form around the implanted films. However, these inflammatory reactions appeared to be a normal host defense mechanism typically presented after surgical implantation. With time, the numbers of neutrophils and giant cells decreased gradually and the capsules became thinner, indicating that acute inflammation has been resolved. Although

there was a slight difference in the levels of inflammatory reactions to the implanted films, no extended acute and chronic inflammation or necrosis was observed. Therefore, the tissue responses in this mouse subcutaneous model strongly suggest that the DMAPS bristle-containing polymers exhibited good biocompatibility. The biocompatibility is most likely due to the hydration characteristics of zwitterionic sulfobetaine bristle end groups present at the PECH-DMAPS40 film surface.

Conclusions

In this study, we synthesized a series of well-defined brush poly(ethylene oxide)s bearing alkyl and sulfobetaine-containing (*i.e.*, DMAPS) bristles in various compositions. These brush polymers were thermally stable up to 185 °C. The brush polymers were found to self-assemble, always forming multi-bilayer structures in films, where the layers stacked along a direction normal to the film plane, regardless of the bristle composition. Due to such multi-bilayer structures, all the DMAPS bristle-containing polymer films provided hydrophilic, zwitterionic sulfobetaine groups at the film surface. The physicochemical properties (water contact angle and water sorption) of the brush polymer films were characterized and correlated with the film morphologies. Films of the DMAPS bristle-containing polymers provided a favorable environment for cell adhesion and revealed biocompatibility in mice, but significantly suppressed protein adsorption. In particular, the suppression of the protein adsorption became much more pronounced in the brush polymer films containing higher contents of DMAPS bristles. Overall, the DMAPS bristle-containing polymers showed excellent biomaterial properties; these properties originated from the hydrophilic, zwitterionic sulfobetaine groups present at the film surface, which were strongly supported by the multi-bilayer structure formed in the film. In summary, the sulfobetaine-containing brush polymers described in this study are suitable for use in biomedical applications, including medical devices and biosensors that require biocompatibility.

Acknowledgements. This study was supported by the National Research Foundation (NRF) of Korea (Basic Research Grant No. 2010-0023396) and the Ministry of Education, Science and Technology (MEST) (Korea Brain 21 Program and World Class University Program (R31-2008-000-10059-0)). The synchrotron X-ray scattering measurements at the Pohang Accelerator Laboratory were supported by MEST and POSCO Company, and POSTECH Foundation.

References

- (1) J. M. Anderson, *Annu. Rev. Mater. Res.*, **31**, 81 (2001).
- (2) J. E. Raynor, J. R. Capadona, D. M. Collard, T. A. Petrie, and A. J. García, *Biointerphases*, **4**, FA3 (2009).
- (3) J. A. Hubbell, *Curr. Opin. Biotechnol.*, **14**, 551 (2003).
- (4) R. Langer and D. A. Tirrell, *Nature*, **428**, 487 (2004).
- (5) B. Zhao and W. J. Brittain, *Prog. Polym. Sci.*, **25**, 677 (2000).
- (6) D. Bozukova, C. Pagnoulle, M.-C. De Pauw-Gillet, S. Desbief, R. Lazzaroni, N. Ruth, R. Jerome, and C. Jerome, *Biomacromolecules*, **8**, 2379 (2007).
- (7) H. Ma, D. Li, X. Sheng, B. Zhao, and A. Chilkoti, *Langmuir*, **22**, 3751 (2006).
- (8) Z. Zhang, T. Chao, S. Chen, and S. Jiang, *Langmuir*, **22**, 10072 (2006).
- (9) G. Kim, L. Y. Hong, J. Jung, D.-P. Kim, H. Kim, I. J. Kim, J. R. Kim, and M. Ree, *Biomaterials*, **31**, 2517 (2010).
- (10) E. Ostuni, R. G. Chapman, M. N. Liang, G. Meluleni, G. Pier, D. E. Ingber, and G. M. Whitesides, *Langmuir*, **17**, 6336 (2001).
- (11) R. G. Chapman, E. Ostuni, M. N. Liang, G. Meluleni, E. Kim, L. Yan, G. Pier, H. S. Warren, and G. M. Whitesides, *Langmuir*, **17**, 1225 (2001).
- (12) S. Chen, J. Zheng, L. Li, and S. Jiang, *J. Am. Chem. Soc.*, **127**, 14473 (2005).
- (13) Z. Zhang, S. Chen, Y. Chang, and S. Jiang, *J. Phys. Chem. B*, **110**, 10799 (2006).
- (14) W. Feng, J. L. Brash, and S. Zhu, *Biomaterials*, **27**, 847 (2006).
- (15) J. Zheng, L. Li, S. Chen, and S. Jiang, *Langmuir*, **20**, 8931 (2004).
- (16) H. Kitano, T. Mori, Y. Takeuchi, S. Tada, M. Gemmei-Ide, Y. Yokoyama, and M. Tanaka, *Macromol. Biosci.*, **5**, 314 (2005).
- (17) Y. Chang, S. Chen, Z. Zhang, and S. Jiang, *Langmuir*, **22**, 2222 (2006).
- (18) A. B. Lowe, M. Vamvakaki, M. A. Wassall, L. Wong, N. C. Billingham, S. P. Armes, and A. W. Lloyd, *J. Biomed. Mater. Res.*, **52**, 88 (2000).
- (19) G. Kim, S. Park, J. Jung, K. Heo, J. Yoon, H. Kim, I. J. Kim, J. R. Kim, J. I. Lee, and M. Ree, *Adv. Funct. Mater.*, **19**, 1631 (2009).
- (20) G. Kim, Y. Rho, S. Park, H. Kim, S. Son, H. Kim, I. J. Kim, J. R. Kim, W. J. Kim, and M. Ree, *Biomaterials*, **31**, 3816 (2010).
- (21) R. J. Huxtable, *Physiol. Rev.*, **72**, 101 (1992).
- (22) (a) J.-C. Lee, M. H. Litt, and C. E. Rogers, *Macromolecules*, **30**, 3766 (1997), (b) J.-C. Lee, M. H. Litt, and C. E. Rogers, *Macromolecules*, **31**, 2440 (1998).
- (23) B. Lee, Y.-H. Park, Y.-T. Hwang, W. Oh, J. Yoon, and M. Ree, *Nat. Mater.*, **4**, 147 (2005).
- (24) B. Lee, W. Oh, Y. Hwang, Y.-H. Park, J. Yoon, K. S. Jin, K. Heo, J. Kim, K.-W. Kim, and M. Ree, *Adv. Mater.*, **17**, 696 (2005).
- (25) B. Lee, J. Yoon, W. Oh, Y. Hwang, K. Heo, K. S. Jin, J. Kim, K.-W. Kim, and M. Ree, *Macromolecules*, **38**, 3395 (2005).
- (26) J. Yoon, K.-W. Kim, J. Kim, K. Heo, K. S. Jin, S. Jin, T. J. Shin, B. Lee, Y. Rho, B. Ahn, and M. Ree, *Macromol. Res.*, **16**, 575 (2008).
- (27) G. Kim, H. Kim, I. J. Kim, J. R. Kim, J. I. Lee, and M. Ree, *J. Biomater. Sci. Polym. Ed.*, **20**, 1687 (2009).
- (28) G. Kim, H. Kim, I. J. Kim, J. R. Kim, J. I. Lee, and M. Ree, *Macromol. Res.*, **16**, 473 (2008).
- (29) S. V. Fulzele, P. M. Satturwar, and A. K. Dorle, *Eur. J. Pharm. Sci.*, **20**, 53 (2003).